

Porous and dense poly(L-lactic acid) and poly(D,L-lactic acid-co-glycolic acid) scaffolds: *In vitro* degradation in culture medium and osteoblasts culture

S. H. BARBANTI^{1,*}, A. R. SANTOS JR.², C. A. C. ZAVAGLIA¹, E. A. R. DUEK^{1,3}

¹Department of Materials Engineering, Faculty of Mechanical Engineering, State University of Campinas (UNICAMP), P.O. Box 6122, 13083-970, Campinas, SP, Brazil
E-mail: samuel@fem.unicamp.br

²Department of Cell Biology, Institute of Biology, State University of Campinas (UNICAMP), Campinas, SP, Brazil

³Department of Physiological Sciences, Faculty of Biological Sciences, Pontifical Catholic University of São Paulo (PUC-SP), Sorocaba, SP, Brazil

The use of bioresorbable polymers as a support for culturing cells has received special attention as an alternative for the treatment of lesions and the loss of tissue. The aim of this work was to evaluate the degradation in cell culture medium of dense and porous scaffolds of poly(L-lactic acid) (PLLA) and poly(D,L-lactic acid-co-glycolic acid) (50:50) (PLGA₅₀) prepared by casting. The adhesion and morphology of osteoblast cells on the surface of these polymers was evaluated. Thermal analyses were done by differential scanning calorimetry and thermogravimetric analysis and cell morphology was assessed by scanning electron microscopy. Autocatalysis was observed in PLGA₅₀ samples because of the concentration of acid constituents in this material. Samples of PLLA showed no autocatalysis and hence no changes in their morphology, indicating that this polymer can be used as a structural support. Osteoblasts showed low adhesion to PLLA compared to PLGA₅₀. The cell morphology on the surface of these materials was highly dispersed, which indicated a good interaction of the cells with the polymer substrate.

© 2004 Kluwer Academic Publishers

1. Introduction

For biological structures that cannot be repaired, the alternative means of re-establishing functions in patients is to use a biomaterial. Implants or transplants are generally used to mimic or to restore the functions of damaged biological structures, but few can fully reproduce all of the complex actions of the original tissue or organ.

Bioresorbable polymer scaffolds are frequently used to stimulate cell growth, proliferation and differentiation. The technique involves the *in vitro* expansion of viable cells obtained from the patient with their subsequent reintroduction into the patient. The polymeric support degrades, peaving only the cells or new tissue [1].

The selection of polymeric materials for tissue engineering follows two basic strategies [2]: First, the synthetic material is developed to physically and mechanically support the cells, from the time of their inoculation up to the formation of premature tissue, which is then implanted in the host organism. In addition to

providing information on cytotoxicity, adhesion and cellular proliferation, cultured cells represent the beginning of recomposition of the natural tissue [3]. Second, implantation occurs when the tissue is preformed. In this case, the polymeric scaffold is developed with mechanical properties and a degradation time appropriate for the inoculation of the cells into a bioreactor where formation of the mature tissue occurs. Both strategies can be used for repairing several types of tissues, with the success of the therapy depending on the type, place and extent of the lesion, and on the biodegradation and bioresorption of the polymeric scaffold [4].

Poly(α -hydroxy acids), such as poly(L-lactic acid) and poly(D,L-lactic acid-co-glycolic acid) are the principal biodegradable and bioresorbable polymers. Biodegradation and bioresorption involve an initial exposure to aqueous fluids, that results in hydration and subsequent hydrolysis of the ester bonds. Degradation results from a gradual loss of the scaffold mass [5–7].

In developing and selecting bioresorbable scaffolds, the degradation time is fundamental for successful

*Author to whom all correspondence should be addressed.

biocompatibility and biofunctionality. Rapid degradation can compromise the mechanical properties whereas an excessively long degradation time can induce chronic inflammatory reactions [8]. Hence, degradation studies often address variables such as the site of the implant [9], the chemistry/stereoisomeric composition of the material [10, 11], crystallinity [12, 13] and the morphology of the scaffold [14, 15].

The conditions investigations of degradation *in vitro* usually try to simulate of physiological pH and osmolarity. Polymeric scaffolds used to culture cells are often maintained in culture medium for up to several weeks. During this time, the material may partially degrade, with alterations in its morphological, thermal and mechanical properties. In this work, we examined the degradation and stability of dense and porous scaffolds of PLLA and PLGA₅₀ kept in culture medium for up to 8 weeks. We also assessed the ability of osteoblasts to adhere to these polymers, and the morphological changes in these cells.

2. Materials and methods

2.1. Scaffold preparation

Membrane scaffolds were prepared using poly(L-lactic acid) (Mw 300,000 Da) and poly(D,L-lactico-glycolic acid) (50:50) (Mw 100,000 Da) supplied by Purac (Groningen, The Netherlands). Dense membranes were prepared using a 10% (w/v) solution of polymer prepared in chloroform (Merck KgaA, Darmstadt, Germany), at room temperature. The membranes were cast on glass plates and dried for approximately 24 h in a closed chamber, with a constant flow of dry, filtered air. Porous membranes were prepared essentially as described above, using a polymer chloroform solution containing 50% (w/v) citrate sodium (Fluka Chemicals, Buchs, Switzerland). Prior to use, the salt was sieved to give particles 180–250 μm in diameter. After casting, the salt was removed by immersion in distilled water for 24 h followed by washing in ethanol for 2 h. The samples were vacuum dried and stored in a desiccator for 5 days to ensure the total removal of solvent.

2.2. Evaluation of degradation *in vitro*

The degradation of dense and porous membranes was studied using Ham-F10 culture medium (Nutricell Nutrientes Celulares, Campinas, SP, Brazil) maintained at $37 \pm 0.5^\circ\text{C}$. The membranes were removed from the medium after 1, 2, 4, and 8 weeks, and washed with distilled water before vacuum drying.

2.2.1. Scanning electron microscopy (SEM)

A JXA 840 scanning electron microscope (Jeol, Peabody, USA), using 10 kV of tension, was used to observe the upper, lower and fracture surfaces. The samples were fractured in liquid nitrogen and coated with gold using a sputter coater SCD 050 Cool Sputter System (Bal-Tec, Balzers, Switzerland).

2.2.2. Thermogravimetric analysis (TGA)

The TGA analysis was carried out in a STA 409C of Netzsch (Gerätebau GmbH Thermal, Selb, Germany). The samples were heated from the room temperature up to 400°C at a heating rate of $10^\circ\text{C}\cdot\text{min}^{-1}$ under helium atmosphere.

2.2.3. Differential scanning calorimetry (DSC)

The measurement of DSC was made while heating the samples from 25 to 200°C at a rate of $10^\circ\text{C}\cdot\text{min}^{-1}$, maintaining the final temperature for 5 min, and then cooling at the same rate; each sample was re-heated. The DSC analysis was carried out in a STA 409C of Netzsch (Gerätebau GmbH Thermal, Selb, Germany). The changes in the glass transition temperature (T_g), crystallization temperature (T_c) and melting temperature (T_m) were evaluate during degradation process. The degree of crystallinity was calculated from the enthalpy change using the equation:

$$\chi(\%) = 100 \times (\Delta H_{\text{melt}} - \Delta H_{\text{crystallization}}) / \Delta H_{100\%}$$

where $\Delta H_{100\%} = 93 \text{ J}\cdot\text{g}^{-1}$ is the enthalpy of melting for 100% crystalline polymer [16].

2.3. Cell culture

OFCOLII cells (a mouse non-transformed osteoblastic line), were obtained from the cell bank at the Federal University of Rio de Janeiro (UFRJ, Rio de Janeiro, Brazil). The cells were cultured in Ham-F10 medium (Nutricell) supplemented with 10% fetal calf serum (FCS, from Nutricell) at 37°C . Cells were seeded onto upper surface of the studied membranes. All of the cell culture assays done were based on standard protocols [17, 18].

2.3.1. Cell adhesion assay

Cell adhesion was studied using the method described in [19] with some modifications. Briefly, the polymers ($n = 6$) were added to 96 well plates (Corning/Costar Corporation, Cambridge, MA, USA) in Ham-F10 for 24 h at 37°C . After this incubation time, $200 \mu\text{L}$ of a cell suspension (1.0×10^5 cell/mL) in Ham-F10 medium containing 10% FCS was added to the wells. The cells were cultured for 2 h at 37°C and then washed with 0.1 mmol/L phosphate buffered saline (PBS) in pH 7.4 at 37°C , before fixing in 10% formalin for 15 min. After washing in PBS, the cells were stained with 0.05% crystal violet (dissolved in 20% methanol) for 15 min, then washed twice with PBS and incubated with 0.1 mmol/L sodium citrate (in 50% ethanol), pH 4.2, for 30 min. The wells were read in a Multiskan Biochromatic microplate reader (Labsystems, Helsinki, Finland) at 540 nm. As a positive control, an empty polypropylene culture plate was read alone. Teflon membranes were used as a negative control. The absorbances of all wells (dense or porous PLLA, dense or porous PLGA, and

negative/positive controls) were also determined without cells as a control for dye staining. For statistical evaluation of the results, a one-way ANOVA was used. Statistical differences among groups were detected by Tukey's *t* test at a 5% level of significant.

2.3.2. Scanning electron microscopy

For morphological analysis, 1.0×10^5 cell/mL were incubated with polymers in Ham-F10 medium supplemented with 10% FCS. Cells cultured on glass coverslips under the same conditions were used as a control. After 24 h, the samples were fixed in 3% glutaraldehyde (Sigma) in 0.1 mmol/L PBS, pH 7.2, for 45 min at 4 °C, and postfixed with 1% OsO₄ for 2 h at 4 °C. The specimens were then dehydrated in an ethanol series, critical point dried (Balzers CDT 030) and coated with gold in a sputter coater (Balzers CDT 050). The coated specimens were viewed and photographed with a Jeol JXA 840 scanning electron microscope. All experiments were done in triplicate.

3. Results and discussion

3.1. Scanning electron microscopy

Samples prepared without the addition of salt had a dense structure, and an irregular upper surface with small concavities (Fig. 1(A)). The lower surface was flat and regular with no pores, because of the contact with the glass plate during casting process. The final morphology is a function of the preparation process, the conditions of solvent evaporation, the degree of crystallinity of the material and the solubility of the polymer in the solvent used. PLLA membranes obtained by casting have similar structures [20]. During the 8 weeks of degradation in Ham-F10 culture medium, there were no significant alterations in the morphology of dense PLLA membranes. For porous PLLA membranes the morphology of the lower surface was similar to that of dense. The upper surface (Fig. 1(B)) was irregular, with concavities generated by the encapsulation of salt particles during evaporation of the solvent, and pores caused by the penetration of water during dissociation and retreat of the salt. The size of the pores (100–200 μm) and the in distribution varied but were lower the size of salt particles used (180–250 μm). After 8 weeks, there was no change in the morphology of the pores or their distribution.

PLGA₅₀ membranes prepared with salt had a morphology similar to that of porous PLLA membranes prior to degradation. The samples had an irregular upper surface with interconnected pores that varied in diameter (150–250 μm) (Fig. 2(A)). After 1 week (Fig. 2(B)), the upper surface was irregular, but had smaller concavities than at time zero. Analysis of the fracture surface confirmed a decrease in the thickness of the material, but maintenance of the pores. These changes were accentuated after 2 weeks. The pores were flattened (Fig. 2(C)) and there was a significant reduction in thickness. After 8 weeks, the morphology was similar to dense PLGA₅₀ membranes (Fig. 2(F)). The fracture surface of dense membranes of PLGA₅₀ showed compactation of the material, with no internal or superficial pores and a regular thickness (Fig. 2(D)). After 1 week, the material had a porous interior (Fig. 2(E)), while the surfaces remained flat and regular. After 8 weeks (Fig. 2(F)) the material lost its membrane form and crowding round. The samples were irregular and showed extensive erosion.

The difference between the morphology of PLLA and PLGA₅₀ membranes during degradation was attributed mainly to the chemical composition and crystallinity of the samples. Hydrolysis generally starts in amorphous regions where there is greater diffusion of water. In a second stage, the crystalline areas begin to degrade. Initially, the degradation occurs principally on the surface because of the absorption gradient of water, but as the concentration of carbonyl groups increases in the center, these serve as catalysts for the process [7, 21, 22]. The autocatalytic effect becomes apparent when one compares dense and porous samples of PLGA₅₀. The smaller the area of diffusion of the degradation products, the larger the effect of the acidic products. Porous membranes have a larger surface area and do not show the internal degradation seen in dense PLGA₅₀ samples after 2 weeks.

The use of salt particles of a controlled size during membrane casting is an appropriate method for producing pores larger than 40 μm [2]. The distribution of the uniformity and interconnection of the pores is fundamental in the production of scaffolds for tissue engineering because these properties facilitate the penetration of fluids through the material and promote the formation of tissue in an organized network. Thus, the morphology of the pores can be regulated by the casting particulate-leaching technique with the use of a

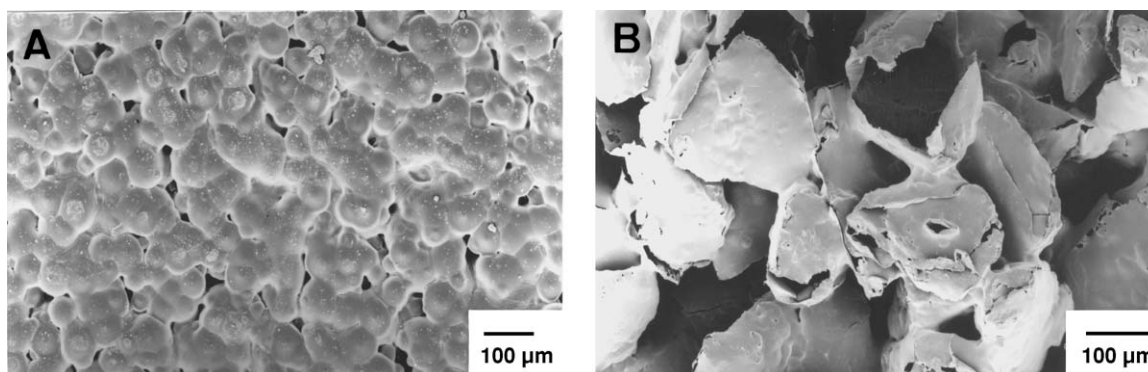


Figure 1 Scanning electron micrographs of PLLA prior to degradation. (A) dense scaffold; (B) porous scaffold; (A), (B) upper surface.

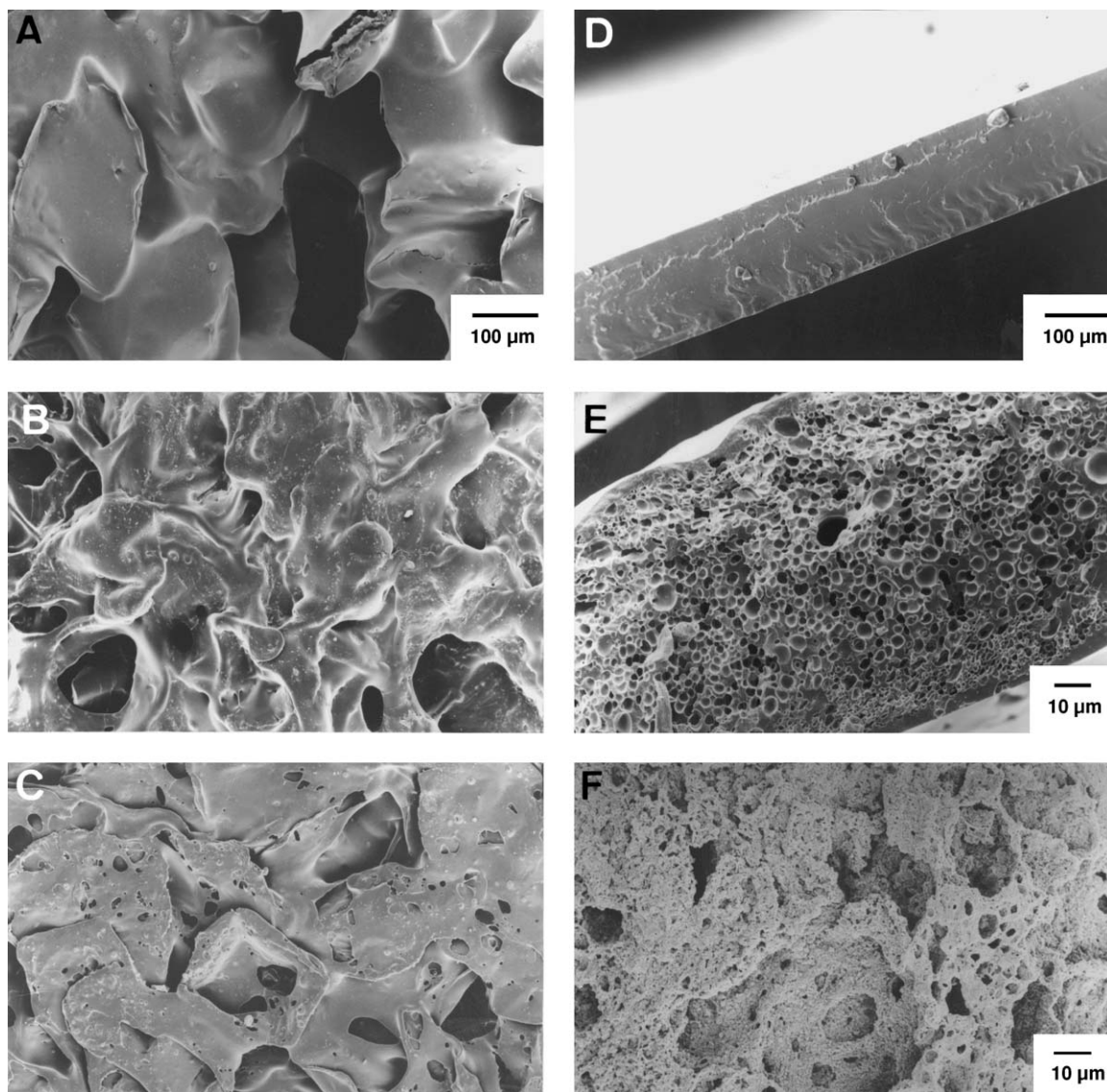


Figure 2 Scanning electron micrographs of PLGA₅₀. Porous scaffolds (A) time zero; (B) 1 week; (C) 2 weeks; Dense scaffolds (D) time zero; (E) 1 week; (F) 8 weeks; (A), (B), (C) upper surface; (D), (E) fracture surface. The scale bar is the same for (A), (B), (C) micrographs.

salt with appropriate characteristics. Variations in the size of the pores do not have a significant influence on the degradation process [20], although the thinner the pore wall, the greater the loss of mass. An autocatalytic effect is observed in materials with thicker pore walls [23].

There were no significant changes in the morphology of porous and dense PLLA membranes. The morphological alterations in dense structures of PLLA depend on the conditions of degradation and on the samples size and thickness. Comparison of our results for degradation in culture medium with other reports in the literature is difficult because latter have frequently used solutions that simulate the conditions of the medium, e.g., PBS. However, studies with PBS indicate similar morphological results during degradation [12, 14].

3.2. Thermogravimetric analysis

Although there were differences in the thermal stability between the samples of PLLA and PLGA₅₀, these did not significantly affect the values of initial temperature of mass loss (Tonset) prior to and after degradation

(Table I). The differences in the Tonset of the materials (PLLA about 345 °C and PLGA₅₀ about 325 °C) were attributed to their composition and crystallinity: the greater the content of lactic acid, and the proximity of the polymeric chains, the greater thermal stability of the material [21]. During degradation, PLLA retained its thermal stability whereas that of PLGA₅₀ decreased markedly (to about 280 °C after 8 weeks of degradation).

TABLE I Thermogravimetric analysis of samples of porous and dense PLLA and PLGA₅₀ as a function of degradation time (weeks)

Weeks	T onset (°C)			
	PLLA		PLGA ₅₀	
	Dense	Porous	Dense	Porous
0	341	348	322	328
1	347	321	302	308
2	349	350	311	311
4	346	338	290	283
8	350	348	281	282

(T onset) initial temperature of loss mass.

Thermal stability is an important factor in the production of bioresorbable material [24]. The physiological temperature at which implants will be used is below their thermal degradation temperature. During heat processing of the material, thermal degradation can generate smaller molecules, as well as products and subproducts of degradation that can interfere with the chemical composition of the material and alter its cytotoxicity and biocompatibility [12].

3.3. Differential scanning calorimetric

Tables II and III show the DSC data. The values obtained for degradation in culture medium were similar to those reported in the literature for degradation in phosphate buffer, pH 7.4. The values for T_g , T_c and T_m for PLLA and PLGA samples before degradation were similar to those obtained here [10, 13, 22]. The T_g and T_m of PLLA were unaltered after 8 weeks in culture medium (Table II). Studies of the long term (36 months) degradation of PLLA films have shown that the T_c and T_g vary with the length of degradation, and begin to decrease after 12 months [25].

The crystallization peak, present only in the second heating of the PLLA samples, suggested that the rate of cooling used ($10^\circ\text{C}\cdot\text{min}^{-1}$) was rapid enough to prevent slow nucleation and crystal growth. Table II shows a tendency of T_c to decrease, probably as a re-

sult of the relaxation of the polymer chains [22]. The PLGA₅₀ samples showed a decline in T_g from the second week onward (Table III). This could reflect the plasticizer effect of water absorbed during degradation [21]. The morphological differences in the PLGA₅₀ membranes were not reflected in variations in the T_g values. After 8 weeks, the material showed crystalline peaks, indicating that there was crystallization of the material. Only for porous membranes of PLGA₅₀ was a crystallization peak observed in the fourth week; this value differed from that observed after 8 weeks (Table III).

The comparison of the morphology of a same material shows that there was no significant effect on the values of T_g , T_c and T_m in the absence of plasticizing agents such as water or solvent. The degree of crystallinity of PLLA samples was calculated from the melting enthalpy (Table II). Crystalline polymers suffer preferential attack in amorphous areas because of greater susceptibility to penetration by water. As a result, the relative percentage of crystalline areas increases as a function of the degradation time [14]. In addition, scission of the chains allows rearrangement to create new crystals [12]. An autocatalytic effect is seen when the relative variation is compared with the degree of crystallinity prior of degradation and after 8 weeks, of the second heating. The dense membranes showed greater variation than the porous membrane, because of their compactness, which made the diffusion of degradation

TABLE II Differential scanning calorimetric data for PLLA samples

PLLA Samples													
Weeks	Heating	T_g ($^\circ\text{C}$)		T_c ($^\circ\text{C}$)		T_m ($^\circ\text{C}$)		ΔH_c (J/g)		ΔH_m (J/g)		χ (%)	
		Dense	Porous	Dense	Porous	Dense	Porous	Dense	Porous	Dense	Porous	Dense	Porous
0	1 $^\circ$	–	–	–	–	178	178	–	–	35	37	37	39
	2 $^\circ$	62	63	111	111	179	180	28	29	36	39	9	11
1	1 $^\circ$	58	62	–	–	180	179	–	–	48	37	51	39
	2 $^\circ$	62	62	105	108	179	178	31	25	66	49	37	26
2	1 $^\circ$	65	56	–	–	180	177	–	–	72	40	77	43
	2 $^\circ$	62	61	106	102	179	179	45	21	100	59	59	41
4	1 $^\circ$	–	–	–	–	178	180	–	–	32	30	34	32
	2 $^\circ$	61	62	105	107	177	179	17	20	38	41	22	22
8	1 $^\circ$	–	–	–	–	178	178	–	–	32	28	34	30
	2 $^\circ$	60	61	102	105	176	177	11	16	31	35	21	20

(T_g) glass transition, (T_c) crystallization and (T_m) melting temperatures, (ΔH_c) crystallization and (ΔH_m) melting enthalpies, (χ) degree of crystallinity.

TABLE III Differential scanning calorimetric data for PLGA₅₀ samples

PLGA ₅₀ Samples													
Weeks	Heat	T_g ($^\circ\text{C}$)		T_c ($^\circ\text{C}$)		T_m ($^\circ\text{C}$)		ΔH_c (J/g)		ΔH_m (J/g)		χ (%)	
		Dense	Porous	Dense	Porous	Dense	Porous	Dense	Porous	Dense	Porous	Dense	Porous
0	1 $^\circ$	–	–	–	–	–	–	–	–	–	–	–	–
	2 $^\circ$	49	49	–	–	–	–	–	–	–	–	–	–
1	1 $^\circ$	46	48	–	–	–	–	–	–	–	–	–	–
	2 $^\circ$	46	48	–	–	–	–	–	–	–	–	–	–
2	1 $^\circ$	47	47	–	–	–	–	–	–	–	–	–	–
	2 $^\circ$	39	47	–	–	–	–	–	–	–	–	–	–
4	1 $^\circ$	–	–	–	–	–	179	–	18	–	–	–	–
	2 $^\circ$	21	31	–	–	–	176	–	21	–	–	–	–
8	1 $^\circ$	31	31	–	–	146	146	31	81	–	–	–	–
	2 $^\circ$	–	–	–	–	157	153	21	39	–	–	–	–

(T_g) glass transition, (T_c) crystallization and (T_m) melting temperatures, (ΔH_c) crystallization and (ΔH_m) melting enthalpies, (χ) degree of crystallinity.

products more difficult. For the PLGA₅₀ samples, the emergence of the crystalline peak can be explained by the rearrangement of the small polymeric chains generated during degradation process, which reorganize to create crystals.

3.4. Adhesion and morphology of osteoblast

Cells cultivated on dense PLLA had a dispersed morphology with extensive intercellular connections (Fig. 4(A)). A similar morphology was observed in control cell (Fig. 4(E)). In porous samples of PLLA, the cells were not as densely packed as in dense membranes (Fig. 4(B)). In dense membranes of PLGA₅₀, the upper surface of the membrane was wrinkled and hindered observation of the cells. This deformation was probably caused during processing of the sample for observation of the cells. The adhered cells had few surface vesicles (Fig. 4(C)) and a similar morphology to that of control cells. The morphological appearance of cells on porous membranes of PLGA₅₀ differed from that on dense membranes. The cells were quite flat with few prolongations (Fig. 4(D)).

Differences were observed in the adhesion of cells to PLLA and PLGA₅₀, but with no significant alterations in surface morphology. Variations in the topography of the dense and porous materials did not affect adhesion. The statistical result ($F = 30.33315$) was significant ($p = 0.000021$). Positive and negative control means are statistically equal to PLGA₅₀ and PLLA samples, respectively. The results are shown in Fig. 3.

The interaction between cells and their substrates depends fundamentally on the surface characteristics of the material. The topography, chemical properties and surface energy determine whether biological molecules they will be adsorbed, thereby influencing the subsequent stages of spreading, proliferation and cellular differentiation [26]. The difference in adhesion between the PLLA and PLGA₅₀ samples was a function of their chemical composition. The adhesion is facilitated by hydrophilic or electrically charge substrates since in these cases the rate of water absorption is greater, thereby increasing the capacity for adhesion. Amorphous scaffolds facilitate cell penetration and tissue vascularization. The absorption of water leads to

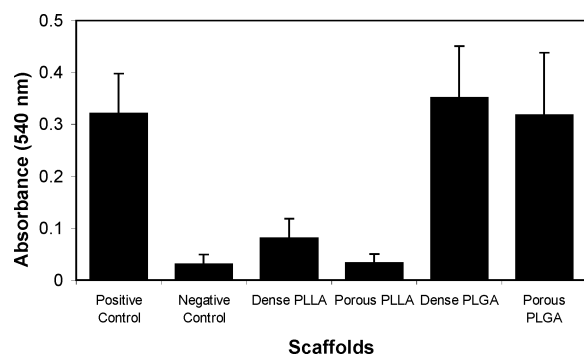


Figure 3 Adhesion of osteoblasts to dense, porous PLLA and PLGA₅₀ scaffolds.

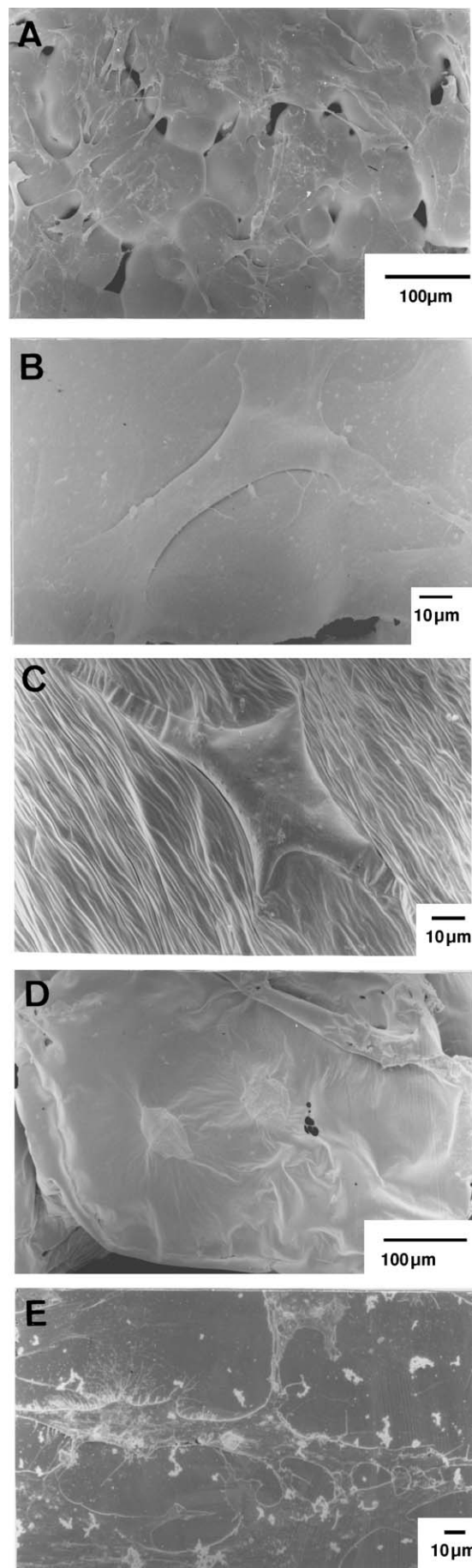


Figure 4 Scanning electron micrographs of osteoblasts on PLLA and PLGA₅₀ scaffolds. (A) cells on dense PLLA; (B) cells on porous PLLA; (C) cells on dense PLGA₅₀; (D) cells on porous PLGA₅₀ and (E) control.

faster degradation compared to crystalline structures, and provides, with pores, the space necessary for tissue invasion [27]. Our results agree with previous studies which also used culture osteoblasts and PLGA₅₀ membranes [28, 29].

The relationship between cell adhesion and cell density suggests that PLLA-based substrates are not as adhesive as those made from PLGA₅₀. Adhesion of the osteoblasts to the PLLA samples was slow. However once attached to the surface of the material, a good interaction of the cells with the substrate was observed. Cellular adhesion, proliferation and differentiation, are inter-related events [26]. Poor cellular adhesion does not necessarily imply low proliferation. Thus, although PLLA membranes are not good adhesive substrates, they can maintain cellular proliferation and stimulate the production of extracellular matrix [3, 30].

Although flat surfaces facilitate adhesion compared to rough ones, the porosity of the scaffold is considered the main criterion for applications in tissue engineering. Pores increase the surface area available for cell invasion and facilitate the diffusion of organic compounds during cell culture, as well as the integration of the material by the host organism [31]. However, increasing the porosity reduces the mechanical properties of the scaffolds and the balance between adhesion and mechanical properties is necessary for the success of the implant [23, 32].

4. Conclusions

Two types of bioresorbable polymers were used in the study. The degradation of the PLGA samples was greater because of the presence of glycolic acid units especially in the dense scaffolds where an autocatalytic effect of the poly(α -hydroxy acids) was seen. Samples of PLLA were stable morphologically for 8 weeks in Ham-F10 culture medium. The thermal stability of the materials was suitable for applications such as a support for cultured cells and there was a relative increase in the degree of crystallinity of the PLLA samples. The PLGA₅₀ samples showed maximum melting after 8 weeks of degradation, indicating crystallization of the material. Cultured osteoblasts adhered best to PLGA₅₀ membranes. Analysis of the cellular morphology suggested a favorable proliferation and differentiation on PLLA samples. These results show that scaffolds of PLLA can be used when a substrate with a prolonged degradation is required to serve as a physical and mechanical support for the cultured cells culture, before and after implantation. Scaffolds of PLGA degrade quickly and may be useful for the formation of mature tissue prior to implantation.

Acknowledgments

This work was supported by The State of São Paulo Research Foundation (FAPESP) (grant 99/05536-7) and The National Council for Scientific and Technological Development (CNPq) (grant 141582/2002-2).

References

1. R. LANGER and J. P. VACANTI, *Science* **260** (1993) 920.
2. D. W. HUTMACHER, *Biomaterials* **21** (2000) 2529.
3. A. R. SANTOS JR, S. H. BARBANTI, E. A. R. DUEK, H. DOLDER, R. S. WADA and M. L. F. WADA, *Art. Org.* **25** (2001) 7.
4. A. ATALA, *J. Endourol.* **14** (2000) 49.
5. M. VERT, M. S. LI, G. SPENLEHAUER and P. GUERIN, *J. Mater. Sci.* **3** (1993) 432.
6. S. A. M. ALI, P. J. DOHERTY and D. F. WILLIAMS, *J. Biomed. Mater. Res.* **27** (1993) 1409.
7. S. LI, *ibid.* **48** (1999) 342.
8. K. A. ATHANASIOU and G. G. NIEDERAUER, *Biomaterials* **17** (1996) 93.
9. J. O. HOLLINGER and G. C. BATTISTONE, *Clin. Ort. Rel. Res.* **207** (1986) 290.
10. D. BENDIX, *Polym. Degrad. Stab.* **59** (1998) 129.
11. R. A. MILLER, J. M. BRADY and D. E. CUTRIGHT, *J. Biomed. Mater. Res.* **11** (1977) 711.
12. E. A. R. DUEK, C. A. C. ZAVAGLIA and W. D. BELANGERO, *Polymer* **40** (1999) 6465.
13. J. C. MIDDLETON and A. J. TIPTON, *Biomaterials* **21** (2000) 2335.
14. K. H. LAM, P. NIEUWENHUIS, H. ESSELBRUGGE, J. FEIJEN, P. J. DIJKSTRA and J. M. SCHAKERAAD, *J. Mater. Sci.: Mater. Med.* **5** (1994) 181.
15. A. G. MIKOS, G. SARA KINOS, M. D. LYMAN, D. E. INGBER, J. P. VACANTI and R. LANGER, *Biotech. Bioeng.* **42** (1993) 716.
16. D. CAM, S. H. HYON and Y. IKADA, *Biomaterials* **16** (1995) 833.
17. C. J. KIRKPATRICK, *Reg. Affairs* **4** (1992) 13.
18. C. J. KIRKPATRICK, F. BITTINGER, H. WAGNER, H. KOHLER, T. C. VAN KOOTEN, C. L. KLEIN and M. OTTO, *Proc. Instn. Mech. Engrs.* **212** (1998) 75.
19. N. MURAKAMI, S. FUKUCHI, K. TAKEUCHI, T. HORI, S. SHIBAMOTO and F. ITO, *J. Cell. Physiol.* **176** (1998) 127.
20. S. H. BARBANTI, C. A. C. ZAVAGLIA and E. A. R. DUEK, *Act. Microsc.* **11** (2002) 85.
21. S. LI, H. GARREU and M. VERT, *J. Mater. Sci.: Mater. Med.* **1** (1990) 342.
22. *Idem.*, *ibid.* **1** (1990) 123.
23. L. LU, S. J. PETER, M. D. LYMAN, H. LAI, S. M. LEITE, J. A. TAMADA, J. P. VACANTI, R. LANGER and A. G. MIKOS, *Biomaterials* **21** (2000) 1595.
24. Y. AOYAGI, K. YAMASHITA and Y. DOI, *Polym. Degrad. Stab.* **76** (2002) 53.
25. H. TSUJI and Y. IKADA, *Polym. Degrad. Stab.* **67** (2000) 179.
26. K. ANSELME, *Biomaterials* **21** (2000) 667.
27. A. G. MIKOS, G. SARA KINOS, M. D. LYMAN, D. INGBER, J. P. VACANTI and R. LANGER, *Biotech. Bioeng.* **42** (1993) 716.
28. S. L. ISHAUG-RILEY, G. M. CRANE, M. J. MILLER, A. W. YASKO, M. J. YASZEMSKI and A. G. MIKOS, *J. Biomed. Mater. Res.* **36** (1997) 17.
29. S. L. ISHAUG-RILEY, G. M. CRANE, M. J. YASZEMSKI and A. G. MIKOS, *Biomaterials* **19** (1998) 1405.
30. C. B. LOMBELLO, A. R. SANTOS JR, S. M. MALMONGE, S. H. BARBANTI, M. L. F. WADA and E. A. R. DUEK, *J. Mater. Sci.: Mater. Med.* **13** (2002) 867.
31. O. M. BÖSTMAN and H. PIHLAJAMAHI, *Biomaterials* **21** (2000) 2615.
32. L. LU, S. J. PETER, M. D. LYMAN, H. LAI, S. M. LEITE, J. A. TAMADA, J. P. VACANTI, R. LANGER and A. G. MIKOS, *ibid.* **21** (2000) 1837.

Received 8 September 2003

and accepted 20 May 2004